



**HAL**  
open science

## Water evaporation versus condensation in hygroscopic soils

Anne-Laure Lozano, Fabien Cherblanc, Jean-Claude Benet

► **To cite this version:**

Anne-Laure Lozano, Fabien Cherblanc, Jean-Claude Benet. Water evaporation versus condensation in hygroscopic soils. *Transport in Porous Media*, 2009, 80 (2), pp.209-222. 10.1007/s11242-009-9351-z . hal-00449660

**HAL Id: hal-00449660**

**<https://hal.science/hal-00449660>**

Submitted on 3 Feb 2011

**HAL** is a multi-disciplinary open access archive for the deposit and dissemination of scientific research documents, whether they are published or not. The documents may come from teaching and research institutions in France or abroad, or from public or private research centers.

L'archive ouverte pluridisciplinaire **HAL**, est destinée au dépôt et à la diffusion de documents scientifiques de niveau recherche, publiés ou non, émanant des établissements d'enseignement et de recherche français ou étrangers, des laboratoires publics ou privés.

# Water evaporation versus condensation in a hygroscopic soil

A.L. Lozano, F. Cherblanc, J.-C. Bénet

Laboratoire de Mécanique et Génie Civil, Université Montpellier 2, CNRS

Place Eugène Bataillon, 34095 Montpellier, France

fabien.cherblanc@univ-montp2.fr

February 3, 2011

## Abstract

The liquid/vapour phase change of water in soil is involved in many environmental geotechnical processes. In the case of hygroscopic soils, the liquid water is strongly adsorbed on the solid phase and this particular thermodynamic state can highly influence the phase change kinetics. Based on the linear Thermodynamic of Irreversible Processes ideas, the non-equilibrium phase change rate is written as a linear function of the water chemical potential difference between the liquid and vapour state. In this relation, the system is characterized by a phenomenological coefficient which depends on the state variables. Using an original experimental set-up able to analyse the response of a porous medium subjected to non-equilibrium conditions, the phase change coefficient is determined in various configurations. This paper focuses on the influence of the gas phase pressure and underlines that a low gas pressure decreases the phase change kinetics. Then, evaporation and condensation processes are compared showing an asymmetric behaviour. These experimental results are interpreted from a microscopic point of view by relying on recent works dealing with molecular dynamics numerical simulation of the liquid/gas interface.

## 1 Introduction

In many geotechnical applications such as water resources management or hazardous waste removal, the liquid/vapour phase change is a central phenomenon. It controls the liquid water availability for agriculture in arid regions and rules the feasibility of a pollution extraction method. In the food industry, the optimization of a drying strategy also depends on water phase change kinetics.

Even, if the phase change necessarily occurs in these applications, its characterization in porous media has received little research attention (Bond and Struchtrup, 2004). Actually, the phase change has generally been considered instantaneous, by supposing that its characteristic time is negligible when compared to other transport phenomena. This is the so-called *local equilibrium* assumption; it results in writing, at the macroscopic scale, that the vapour partial pressure is always equal to its equilibrium value defined by the saturating vapour pressure and desorption isotherm curves. Many water transport models have been built on this assumption, leading to predicted water content profiles in agreement with experimental observations (Whitaker, 1977; Moyne and Perre, 1991; Couture et al, 1995; Prat, 2002). Nevertheless, these models have been applied to describe the water transport when its thermodynamic state is governed by capillary forces, i.e., in the pendular domain. At low water content, hygroscopic effects become predominant and some experimental observations have highlighted that the adsorptive interactions drastically decrease the phase change kinetics (Armstrong et al, 1994; Ruiz and Bénet, 2001; Chamhari et al, 2008; Lozano et al, 2008). In these situations, the phase change is not fast enough to maintain the equilibrium between liquid and gas phases, so that the *local equilibrium* assumption should be called into question.

At the microscopic scale of the liquid/gas interface, the phase change flux is generally represented by the Hertz-Knudsen law derived from the kinetic theory of gases (Eq. 9). From an experimental point of view (Eames, 1997; Bedeaux and Kjelstrup, 1999; Fang, 1999; Marek and Straub, 2001) or using molecular dynamics numerical simulation (Matsumoto, 1998; Meland et al, 2003; Kjelstrup et al, 2008), a large amount of research have been done to test the validity of this law, and to evaluate the weighting coefficient,  $\epsilon$ . So far, the influence of adsorptive forces has not been investigated, although they can significantly modify the physical properties of water (Skipper, 1998; Park and Sposito, 2002; Porion et al, 2007).

At the macroscopic scale, the phase change phenomenon appears as a coupling term,  $J$  ( $\text{kg m}^{-3} \text{ s}^{-1}$ ), between the liquid and gas mass balance equations:

$$\frac{\partial \rho_l}{\partial t} = -\nabla \cdot (\rho_l \mathbf{v}_l) - J \quad (1)$$

$$\frac{\partial \rho_v}{\partial t} = -\nabla \cdot (\rho_v \mathbf{v}_v) + J \quad (2)$$

This phase change rate,  $J$ , is not equivalent to the microscale phase change flux since it encapsulates various microscale phenomena such as interfacial phase change, vapour diffusion, liquid surface diffusion, thermal conduction, ... However, the coupled behaviours of these multiple phenomena and their dependencies on the hygroscopic effects have not been clearly established. Therefore, developing a macroscopic phase change relation using an upscaling technique is out of reach since the microscopic problem is not well defined. An alternative is to address this issue by means of a macroscopic phenomenological approach and rely on the Thermodynamic of Irreversible Processes ideas. In this framework, the soil/water system is characterized by a phenomenological coefficient that must be determined experimentally.

Previous experimental investigations have dealt with the evaporation of water and heptanes in a clayey silty sand (Bénet and Jouanna, 1982; Ruiz and Bénet, 2001; Lozano et al, 2008). These works have clearly shown that the phase change rate in a hygroscopic soil is *not* infinite, and have underlined the influence of the liquid content, temperature and soil texture on the evaporation kinetics.

Concerning the transport phenomena in porous media, symmetric behaviours are classically observed, i.e., an identical phenomenological coefficient is obtained by reversing the generalized force that causes the thermodynamic flux. At this point, our goal is to investigate and compare the evaporation and condensation behaviours. In order to help the interpretation of these experimental results at the microscopic scale, the dependence of phase change kinetics on the total gas pressure is also analyzed.

For the readability of this paper, the basic ideas used to develop the phenomenological relation of non-equilibrium phase change are summarized in the next section. Then, the materials, methods and data processing are described. Finally, the experimental results are presented and discussed from a microscopic point of view.

## 2 Macroscopic model of phase change phenomenon

From a macroscopic point of view, a heterogeneous system is constituted of several superimposed continua in each of which classical continuum thermodynamic applies with additional source/sink terms accounting for the interactions between them. Focusing on unsaturated soils leads to consider three continua: an undeformable solid phase composed of grains, a liquid phase all-water partially adsorbed on the solid structure and a gas phase compounded of dry air and water vapour. Developing the mass, momentum, energy and entropy balances allows us to identify the internal production rate of entropy,  $\chi$  ( $\text{J K}^{-1} \text{ m}^{-3} \text{ s}^{-1}$ ). The part due to phase change is:

$$\chi = J \frac{\mu_l - \mu_v}{T} \geq 0 \quad (3)$$

where,  $J$ , is the volumetric phase change rate ( $\text{kg m}^{-3} \text{ s}^{-1}$ ),  $\mu_l$  and  $\mu_v$  are, respectively, the mass chemical potential of water and its vapour ( $\text{J/kg}$ ), and  $T$  is the temperature. This entropy source

is written as the product of a thermodynamic flux,  $J$ , with a generalized force,  $\mu_l - \mu_v$ . This means that the phase change rate results from a water chemical potential difference between its liquid state,  $\mu_l$ , and its vapour state,  $\mu_v$ . The principles of linear TIP (Thermodynamic of Irreversible Processes) assert that, close to an equilibrium state, the phase change rate,  $J$ , depends linearly on the associated force by writing:

$$J = L \frac{\mu_l - \mu_v}{T} \quad (4)$$

The phenomenological coefficient,  $L$  (kg K s m<sup>5</sup>), introduced in this relation characterizes the system under investigation, i.e., it depends on the state variables (temperature,  $T$ , gas pressure,  $P_g$ , water content,  $w$ , ...) but also on the materials characteristics (nature of the fluid, porous medium texture, ...).

The liquid chemical potential,  $\mu_l$ , must be thought at the macroscopic scale as an homogenized potential. In the case of liquid water in soils, it mainly represents the hygroscopicity resulting from adsorptive and capillary forces. Moreover, with clayey materials, electrical surface charges entails particular ionic distributions generally described by the electrical double-layer theory (Mitchell, 1993). These additional electrostatic interactions also participate to the binding energy between the liquid water and the solid structure (Leroy et al, 2007). These pore-scale interactions are measured at the macroscopic scale through the desorption isotherm that gives the water activity as a function of the water content (Fig. 1). This allows one to determine the equilibrium partial vapour pressure,  $P_{veq}$ , as a function of the water content by:

$$P_{veq} = a(w, T) P_{vs}(T) \quad (5)$$

where  $P_{vs}$  is the saturating vapour pressure and  $w$  is the water content defined by the ratio of the liquid phase apparent density,  $\rho_l$ , divided by the solid phase apparent density,  $\rho_s$ .

In the general non-isothermal case, Bénet and Jouanna (1982) have shown that Eq. 4 can be rewritten as a function of experimentally attainable quantities like the vapour pressures, leading to (Ruiz and Bénet, 2001):

$$J = J_{eq} + L \frac{RT}{M} \ln \left( \frac{P_v}{P_{veq}} \right) \quad (6)$$

where  $R$  is the ideal gas constant (J mol<sup>-1</sup> K<sup>-1</sup>),  $M$  is the liquid phase molar mass (kg mol<sup>-1</sup>). It is written as the sum of an equilibrium part,  $J_{eq}$ , and a non-equilibrium part. The equilibrium part accounts for the phase change resulting from temperature variations while the liquid water remains in equilibrium with its vapour. For instance, it represents the water quantity that evaporates during a temperature raise to maintain the saturating vapour pressure in the gas phase. It generally relates to slow or quasi-static phenomena. On the opposite, the non-equilibrium part characterizes the response of the system to a non-equilibrium situation. This non-equilibrium is taken into account by a deflection of the vapour pressure,  $P_v$ , with respect to its equilibrium value,  $P_{veq}$ .

This relation has been experimentally validated in the case of water and heptanes in a soil (Ruiz and Bénet, 2001; Chammari et al, 2003) It has emphasized the existence of a linear domain close to equilibrium where the phase change coefficient,  $L$ , is constant. A non-linear formulation has been proposed to investigate situations occurring far from equilibrium (Lozano et al, 2008). So far, the influences of water content, temperature, soil texture and liquid nature have been underlined. In order to compare the evaporation and condensation kinetics, the soil under investigation and the experimental methods are detailed in the next section.

### 3 Material and Methods

This section deals with the experimental determination of the phenomenological coefficient  $L$  introduced in Eqs. 4 and 6. With this objective, the phase change phenomenon must be activated in a soil sample, large enough to be considered as a Representative Elementary Volume. To isolate this phenomenon from other transport phenomena (diffusion, convection, ...), it requires the uniformity of the soil state variables (porosity, temperature, water content, ...). The experimental

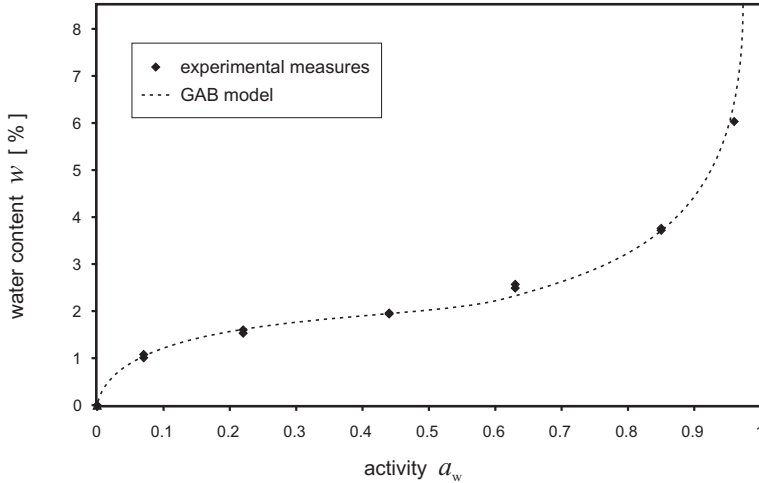


Figure 1: Desorption isotherm of the Clayey Silty Sand at  $T = 30^\circ C$ .

principle consists in changing instantaneously the composition of the gas phase inside the soil sample, in order to create a non-equilibrium between the liquid water and its vapour. Substituting by a gas phase with a vapour pressure lower than its equilibrium value,  $P_{veq}$ , stimulates the water evaporation, while using a gas phase with a vapour pressure greater than its equilibrium value leads to water condensation. The return back to equilibrium manifests itself by a total gas pressure increase in the case of evaporation, or a decrease when condensation occurs. Analysing this return to equilibrium allows us to determine the phase change rate represented by the coefficient,  $L$ .

The soil under investigation is a clayey silty sand, from the bank of the Hérault river (south of France). This soil is classified as SC-CL according to the USCS. The liquid and plastic limits are respectively 25% and 14.5%. Sand, silt and clay fraction are 72%, 18% and 10% respectively (Saix et al, 2000). The organic matter content has been found to be negligible. The clayey fraction, although existing in a small proportion, plays a predominant role with respect to the water retention characteristics. This point is emphasized by the desorption isotherm that gives the water content as a function of the activity (Fig. 1).

The complete experimental device is presented in Fig. 2. The soil is first dried at  $105^\circ C$  for 24 hours. The required amounts of soil (18 g) and distilled water are added using a high-precision balance ( $10^{-4}$  g). After mixing, it is stored in a waterproof container for 24 hours to ensure the homogeneity of the water content. Then, the wet soil is compacted in a cylindrical ring (a) (32 mm diameter and 15 mm thick) by means of a hydraulic press in order to reach a dry density of  $1500 \text{ kg m}^{-3}$ , which corresponds to a porosity of 43% (Fig. 2).

The pressure and temperature sensor (b) is autonomous and programmable (type NanoVACQ from TMI Orion, Montpellier, France). On the left side, a vacuum pump linked to a pressure controller holds the absolute pressure in the vacuum vessel (c) at 10 kPa. On the right side, a large volume of air is regulated at a fixed hygrometry by using saline solutions: potassium sulphate for  $RH = 97\%$  or potassium hydroxide for  $RH = 7\%$ . A three-way valve (d) allows us to, first, put the soil sample in contact with the vacuum vessel, second, connect the soil sample with a controlled hygrometry air, and then, completely isolate the sample. The whole device is placed in a thermo-regulated bath (f) in order to maintain a constant temperature,  $T = 30^\circ C$ .

The experimental process includes three steps (Fig. 3):

- Phase 1 - Thermal equilibrium: The device and sample are put in the thermo-regulated bath for one hour until thermal equilibrium is obtained.
- Phase 2 - Replacement of the gas phase: For 3 seconds, the soil sample is connected to the vacuum vessel through the valve, and then connected to the hygrometry controlled air for

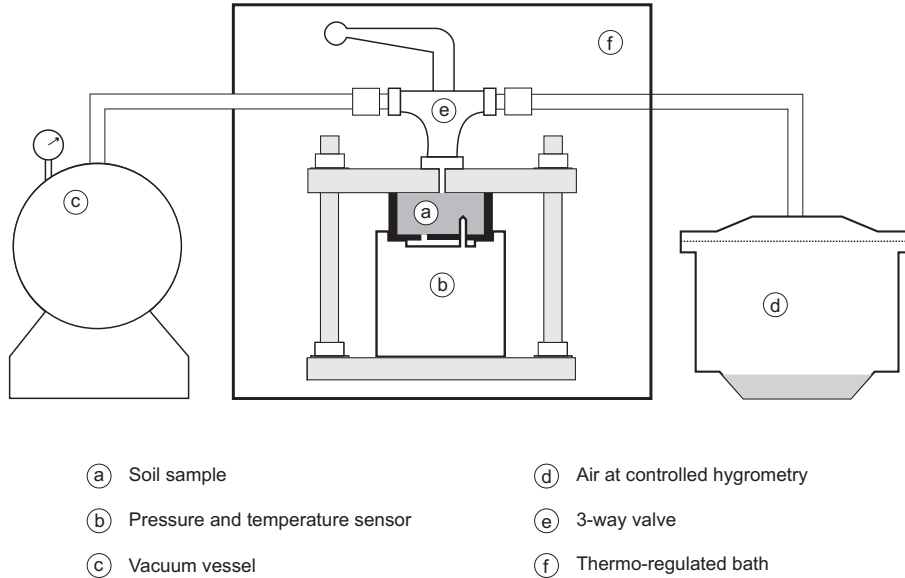


Figure 2: Experimental device for the determination of the phase change coefficient,  $L$ .

another 3 seconds. This stage aims to create the thermodynamic non-equilibrium between the liquid phase and its vapour. With respect to the time required for the whole experiment, this phase is considered instantaneous.

- Phase 3 - Return to equilibrium: After closing the valve, the soil sample is completely insulated and evolves as a thermodynamically closed system in isothermal conditions. The temperature,  $T$ , and total gas pressure,  $P_g$ , are recorded during this phase.

The experimental procedures concerning evaporation and condensation differs only by the characteristics of the injected air, dry air,  $RH = 7\%$ , to activate evaporation and saturated moist air,  $RH = 97\%$ , to activate condensation.

Since the gas phase re-injected after extraction is at the atmospheric pressure, this method enables analysing the phase change occurring in normal conditions. Showing the influence of the total gas pressure on phase change kinetics would bring some interesting details on pore-scale phenomena. With this objective, the evaporation process can be activated with a gas phase pressure below the atmospheric pressure. Experimentally it consists in, during the phase 2, extracting only a fraction of the gas phase by regulating the pressure of the vacuum vessel ((c) in Fig. 2), and let the system evolves in closed conditions. Thus, the partial vapour pressure in the pores drops below its equilibrium value stimulating the bulk evaporation phenomenon.

Next section presents some raw data obtained from this experimental procedure and the processing method allowing us to determine the phase change phenomenological coefficient,  $L$ .

## 4 Data processing

Some examples of the temperature,  $T$ , and the total gas pressure,  $P_g$ , evolutions are presented in Figs. 3a and 3b for one evaporation test at the atmospheric pressure, i.e., dry air at atmospheric pressure is re-injected after gas phase extraction, in a soil sample at  $w=3\%$ . In Fig. 3a, one can see a small temperature drop-down in phase 2. This stems from the fast extraction of the gas phase; the evaporation induced cools down the liquid interfaces. To avoid these temperature fluctuations and to satisfy the isothermal conditions assumed in the theoretical development of the phase change relation, the experimental data are processed between  $t_0$  and  $t_{eq}$ . In this time interval,

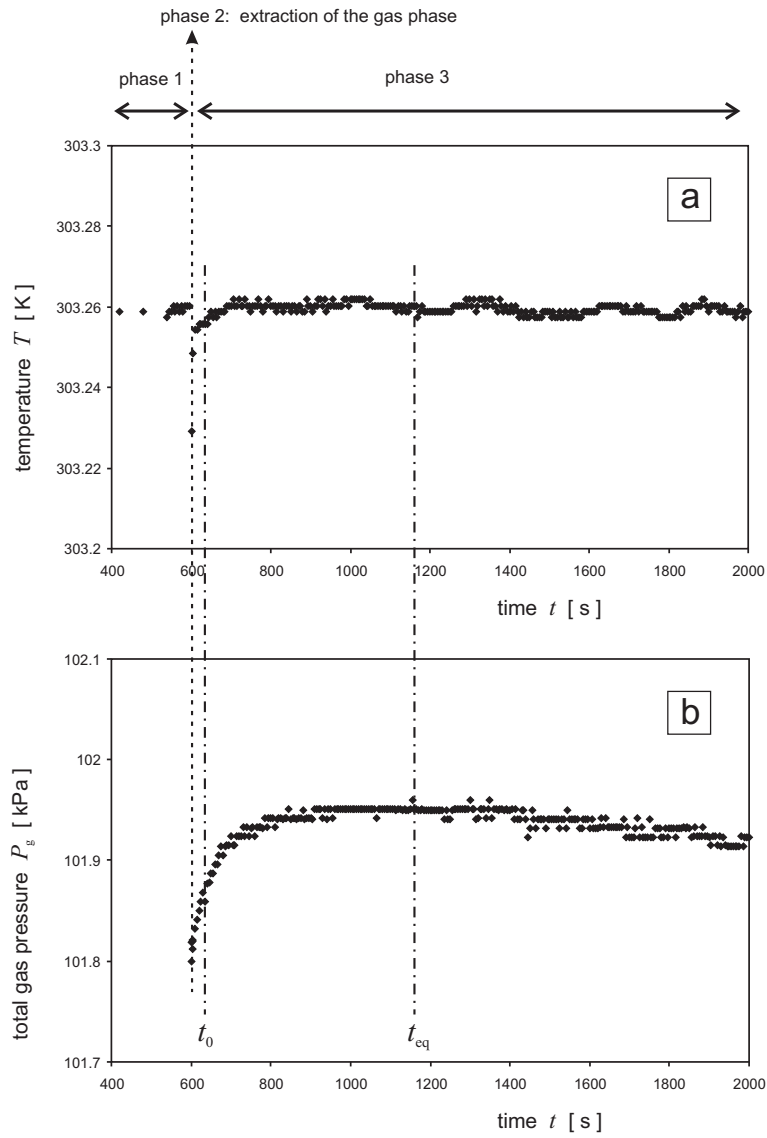


Figure 3: Temperature and pressure evolutions for the evaporation process experiment in soil sample at  $w=3\%$ ; a) Temperature,  $T$  - b) Total gas pressure,  $P_g$

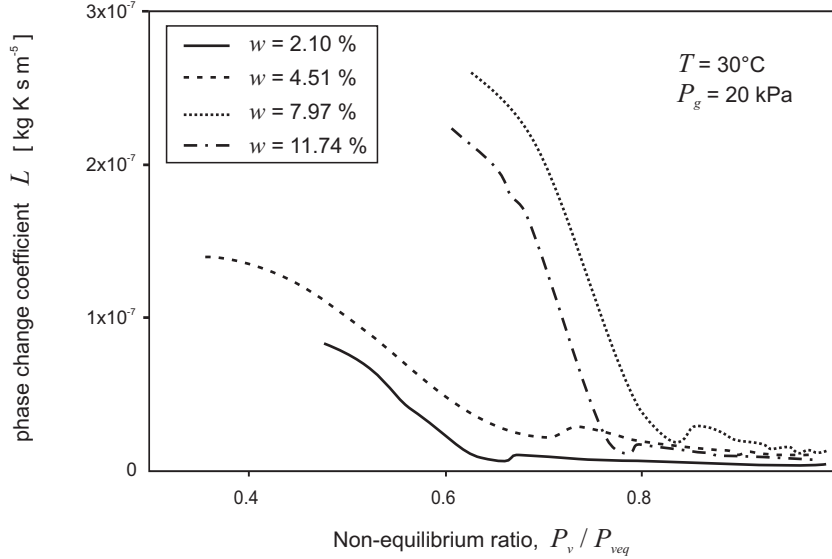


Figure 4: Evolutions of the phenomenological coefficient versus  $P_v/P_{veq}$  at  $T = 30^\circ C$  and various water contents,  $w$ .

the phase change mass rate is slow enough to consider that the macroscopic thermal equilibrium is fairly satisfied. One can see in Fig. 3b that the gas pressure increases about  $\Delta P_g = 200$  Pa. Next to the reinjection of dry air ( $RH = 7\%$ ), the initial vapour pressure is theoretically  $P_v = 1092$  Pa. Since the equilibrium vapour pressure given by Eq. 5 at  $w = 3\%$  is  $P_{veq} = 3340$  Pa, the experimental pressure increase could be around  $\Delta P_g = 2200$  Pa, which is much larger than the measured variation. This means that the first seconds of the evaporation process cannot be caught since the phase change rate is too high at the beginning.

Since homogeneous phase change is activated, the convective fluxes are cancelled. In isothermal conditions, the equilibrium phase change,  $J_{eq}$ , involved in Eq. 6 can be discarded. Using the ideal gas model, the vapour mass balance equation is written as:

$$\frac{\partial P_v}{\partial t} = L \frac{R^2 T}{\eta_g M^2} \ln \left( \frac{P_v}{P_{veq}} \right) \quad (7)$$

where  $\eta_g$  is the volume fraction of the gas phase, which can be considered constant since the volume of liquid water evaporated during one experimental test is negligible.

Assuming that the moist air behaves as an ideal gas mixture, the total gas pressure,  $P_g$ , given in Fig. 3b is the sum of the vapour pressure,  $P_v$ , and the dry air pressure,  $P_a$ . During the phase 3, the soil sample is a closed system at a constant temperature. Therefore, the amount of dry air in the pores remains constant throughout the entire experiment, and its partial pressure,  $P_a$ , is evaluated at the final equilibrium when the partial vapour pressure,  $P_v$ , equals its equilibrium value,  $P_{veq}$ :

$$t \rightarrow \infty \quad ; \quad P_a = (P_g)_{t \rightarrow \infty} - P_{veq} \quad (8)$$

Thereby, the vapour pressure evolution deduced from experimental data is numerically smoothed using a Savitsky-Golay algorithm (Press et al, 1992), before computing the time derivative that appears in Eq. 7. This relation allows us to determine the phase change coefficient,  $L$ , at each time step. In the phase change relation (Eq. 6), the ratio of the vapour pressure divided by its equilibrium value,  $P_v/P_{veq}$ , is related to the thermodynamic force that governs the phase change phenomenon. It can also be seen as a non-equilibrium criterion indicating the experimental conditions: *far from* or *close to* equilibrium. From that perspective, the phenomenological phase-change coefficient,  $L$ , is plotted as a function of this non-equilibrium criterion in Fig. 4.



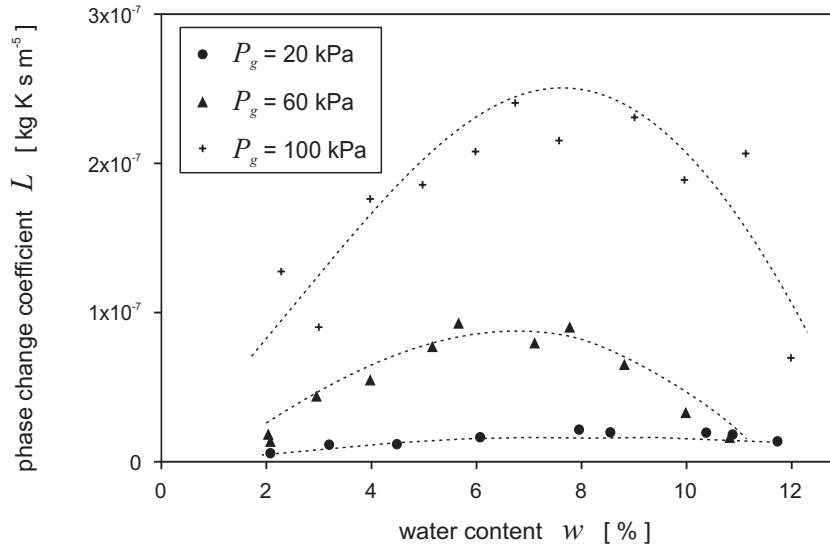


Figure 5: Comparison of the phase change coefficients,  $L$ , in the case of evaporation for various total gas pressure,  $P_g$ . The dashed lines are given for indication.

One can clearly discriminate a domain close to equilibrium where the phase change coefficient,  $L$ , is nearly constant. This defines the validity domain inside which the linear TIP applies, since phenomenological coefficients are assumed to be independent of the thermodynamic forces (Kuiken, 1994). The linearity in a neighbourhood of equilibrium has already been observed using a different data processing method (Bénet and Jouanna, 1982; Ruiz and Bénet, 2001). Below this limit, as non-equilibrium increases, a non-linear behaviour is observed, while the phase change kinetics is strongly enhanced. This aspect has been investigated by Lozano et al (2008) and is beyond the scope of this paper.

In the next section, we focus on the equilibrium value of the phase change coefficient, i.e., the averaged value in the domain close to equilibrium. The influence of various state variables are analysed, evaporation and condensation cases are compared.

## 5 Experimental results

To emphasize the microscopic phenomena involved in the phase change, the phase change coefficient,  $L$ , is determined for a wide range of water content,  $w$ . For the three gas pressures investigated,  $P_g=20$  kPa, 60 kPa and 100 kPa, the results are gathered in Fig. 4. In the case of evaporation, the humidity of dry air injected is  $RH = 7\%$ . To obtain a non-equilibrium large enough to be measurable, the water activity must be greater than 0.5, what corresponds to a water content,  $w > 2\%$  (Fig. 1). Consequently, the water content range investigated lies between 2% and 12%. Above 12%, the gas phase is occluded and phase change cannot be observed.

When representing the phase change coefficient as a function of the water content, a classical bell-shaped curve has always been observed (Bénet and Jouanna, 1982; Ruiz and Bénet, 2001; Lozano et al, 2008). The phase change coefficient reaches a maximum around  $w = 7\%$ , which is roughly the upper limit of the hygroscopic domain (Fig. 1). Below this maximum, when hygroscopic effects become predominant, the intensity of solid-liquid interactions increases in the adsorbed water layers. The supplementary energy requires for water desorption decreases the phase change kinetics, leading to a lower phase change coefficient,  $L$ . Above this maximum, hygroscopic effects are negligible and the water is in a “free” state. As the water content increases, the phase change kinetics decreases since the liquid-gas interface is getting lower.

It must be noted that the gas phase is mainly composed of dry air. Therefore, the results presented in Fig. 5 clearly demonstrate the dependence of evaporation kinetics on the air pressure. Even if the case of evaporation in a low pressure gas is not practically encountered, this could bring some interesting features regarding to the pore-scale phenomena. This issue is discussed in term of interfacial evaporation process in the last section.

Symmetrically, the condensation phenomenon is activated by injecting saturated moist air in the pore space. Using a potassium sulphate solution, the relative humidity imposed is  $RH = 97\%$ . For one condensation experiment, the temperature,  $T$ , and gas pressure,  $P_g$ , measured are plotted versus time in Fig. 6. Alike in the evaporation case (Fig. 3), a small temperature drop is observed (Fig. 6a). It corresponds to the gas extraction stage that generates pore-scale evaporation and liquid-gas interface cooling. In the third phase, the gas pressure decreases while vapour condensates, and tends toward an equilibrium state. The time required to reach an equilibrium ( $\approx 50$  s) is considerably lower than observed in the evaporation process ( $\approx 500$  s). Consequently, the phase change coefficient in condensation is greater than in evaporation, as presented in Fig. 7

To create a significant non-equilibrium between the water and the vapour injected, the water activity must be lower than 0.5, what corresponds to a maximum water content,  $w < 2\%$  (Fig. 1). Therefore, both evaporation and condensation tests cannot be carried out on a same soil sample and the two plots presented in Fig. 7 cannot spread over the whole water content range. Anyway, comparing both phase change processes shows that the condensation phenomenon is about 20 times faster than the evaporation phenomenon.

In our sense, this asymmetric behaviour between evaporation and condensation does not result from the hysteresis inherent to the adsorption/desorption curves (Gawin et al, 2001). Indeed, the hygroscopicity and the phase-change characteristics are intimately related as shown in Fig. 5. However these two characteristics are not of the same kind since the first one qualifies an equilibrium situation while the second one describes the kinetics resulting from non-equilibrium conditions. Nevertheless, asymmetry and hysteresis may indicate that, at the pore-scale, the evaporation and condensation sites are not identical leading to different water distribution and different transport characteristic times as discussed in the next section.

## 6 Discussion

The experimental results presented above can be summarized under the following items:

- The hygroscopic effects decreases the phase change kinetics. This point has also been underlined in Lozano et al (2008) where the clayey fraction of two different soils has been correlated to the evaporation kinetics.
- Increasing the total gas pressure leads to enhance the phase change rate.
- Condensation phenomenon runs faster than evaporation.

These observations can be discussed by relying on two different point of views, at the macroscopic or microscopic scale.

From the microscopic point of view, phase change phenomenon takes place near the liquid-gas interface. For one hundred years, intensive research has been done about modelling the evaporation/condensation flux at the interface scale. Theoretically derived from the kinetic theory of gases, the Hertz-Knudsen law defines the interfacial flux,  $J_{inter}$ , as:

$$J_{inter} = \epsilon (P_{vs} - P_v) \sqrt{\frac{M}{2\pi RT}} \quad (9)$$

Many researches have focused on the evaluation of the evaporation coefficient,  $\epsilon$ . For water, experimentally measured values have ranged from 0.001 to 1 and it is, therefore, understandable that this coefficient has been the subject of much speculation over the last 60 years, as extensively reviewed by Eames (1997). For instance, some experimental results show that this correction

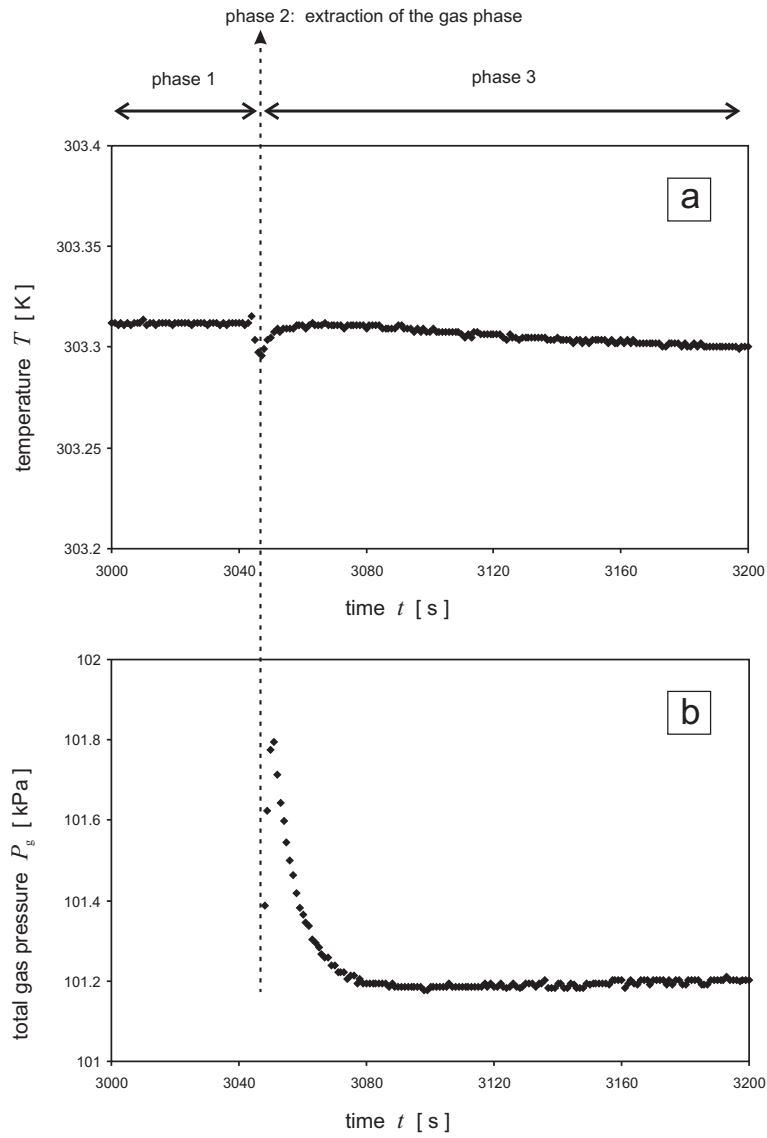


Figure 6: Temperature and pressure evolutions for the condensation process experiment; a) Temperature,  $T$  - b) Total gas pressure,  $P_g$

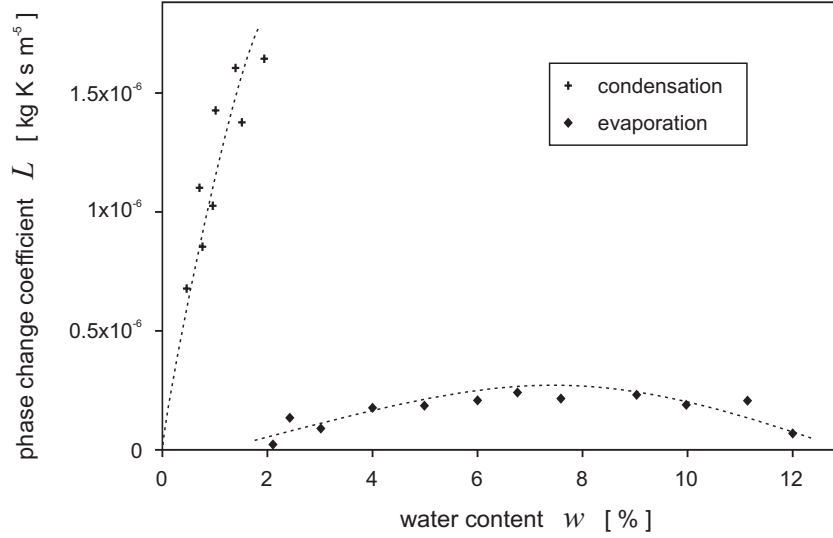


Figure 7: Comparison of the phase change coefficients,  $L$ , measured in the cases of condensation and evaporation at atmospheric pressure

coefficient is higher in the case of condensation than for evaporation (Marek and Straub, 2001), in agreement with the results presented in Fig. 7.

Recently, thanks to the increasing computing facilities, numerical simulations of microscale phase change have been performed using molecular dynamics approaches. This allows examining the physical quantities that govern the phase change at the scale of a water molecule. In particular, one evaporation mechanism, identified as “molecular exchange” or “stimulated evaporation”, relates to the evaporation of a water molecule resulting from the collision with a molecule of the gas phase (Yasuoka et al, 1995; Matsumoto, 1998). The case of water evaporation in air has not been investigated. Nevertheless, Matsumoto (1998) have shown that, with associating fluids like water, molecular exchange becomes a predominant mechanism. This feature could account for the dependence of evaporation kinetics on total gas pressure shown in Fig. 4. Indeed, a higher gas pressure means more interfacial collisions between water and air molecules and leads to increase the stimulated evaporation flux. Using a similar numerical approach, Meland et al (2003) have calculated the evaporation and condensation coefficients, showing that they are not equal outside equilibrium. This agrees with our experimental observation underlining that evaporation and condensation in porous media are not symmetric phenomena.

The microscopic origin of hygroscopicity must be sought at the liquid-solid interface, where surface forces develop. At this scale, the water molecules are adsorbed on the solid phase by short-range interactions like van der Waals or electrostatic forces, and cannot be considered to be in a “free” state. This water-solid binding energy can be evaluated using the chemical potential of the water phase. The chemical potential difference between an adsorbed state and a “free” state is given by:

$$E_b = \Delta\mu = \mu_{free} - \mu_{adsorbed} \quad (10)$$

$$= \mu_l^0 + \frac{RT}{M} \ln \left[ \frac{P_{vs}}{P^0} \right] - \left( \mu_l^0 + \frac{RT}{M} \ln \left[ \frac{P_{veq}}{P^0} \right] \right) \quad (11)$$

$$= -\frac{RT}{M} \ln \frac{P_{veq}}{P_{vs}} \quad (12)$$

$$= -\frac{RT}{M} \ln [a(w, T)] \quad (13)$$

This binding energy,  $E_b$ , is directly related to the activity of water,  $a(w, T)$ , given by Fig. (1). For a water content of 2% the water activity is 0.45, what corresponds to a binding energy,  $E_b = 112$  kJ/kg. It seems to be negligible when compared to the latent heat of vaporization,  $L_v = 2260$  kJ/kg, but is of the same order of the molecular thermal kinetic energy at  $T = 30^\circ C$ ,  $E_T \approx 150$  kJ/kg. Thus, we can fairly infer that this additional energy required for evaporation may impede the phase change, and decrease the phase change coefficient. At the molecular scale, numerical simulations have confirmed that the physical properties of water in clay aggregates are significantly modified by the presence of solid/liquid interactions (Skipper, 1998; Park and Sposito, 2002; Porion et al, 2007). With respect to transport phenomena, this adsorbed water does not behave like bulk water, as experimentally observed in this work regarding to the evaporation process.

At the macroscopic scale, transport phenomena in porous media are generally symmetric, what means that reversing the force causes an opposite flux while keeping the same proportionality between them. This is obviously the case concerning transport phenomena involving only one phase such as molecular diffusion or thermal conduction, but not necessarily with phenomena describing exchanges between phases, as observed in this work. Actually, a macroscopic mass exchange between phases generally accounts for various micro-scale transport phenomena. Indeed, during one evaporation experiment, the soil/water system response to a non-equilibrium situation is obtained through the liquid/gas interfacial evaporation and also through the homogenization of vapour pressure by diffusion, the thermal balancing resulting from interface cooling, the surface diffusion from bounded water to “free” water, ... Therefore, the evaporation and condensation processes do not necessarily involve identical microscopic transport phenomena and similar characteristic times.

Moreover, a natural soil is an extremely heterogeneous medium at multiple scales. The clayey fraction creates some very fine porous aggregates ( $\approx 0.1 \mu m$ ) embedded in a larger heterogeneous structure made of sand grains ( $\approx 100 \mu m$ ) (Mitchell, 1993). With clayey silt at low water content, a double-porosity structure is often encountered (Delage et al, 1996). In this situation, evaporation and condensation sites could be different and may explain the observed asymmetric behaviour.

## 7 Conclusion

The water phase change occurring in hygroscopic soils has been investigated at the macroscopic scale. Based on a thermodynamic macroscopic description of unsaturated porous media, a homogenized relation of non-equilibrium phase change is proposed. It emphasizes the generalized force that governs the phase change in term of the chemical potential difference between the liquid and vapour state. In this relation, the phase change kinetics is characterized by a phenomenological coefficient that must be determined experimentally.

In that objective, an experimental set-up has been developed allowing analysing the dependence of the phenomenological coefficient on various state variables. Thereby, the influence of the gas pressure is presented showing faster evaporation processes when the gas pressure is increased. Then, evaporation and condensation phenomena are compared bringing out the non-symmetric behaviour of phase change.

These experimental results emphasize the major role plays by hygroscopic effects that can considerably decrease the phase change kinetics. In such hygroscopic materials, the *local equilibrium* assumption classically used in drying models could be called into question. When dealing with water transport at low water content, the phase change phenomenon could become a key phenomenon that should be adequately represented.

## References

- Armstrong J, Frind E, McClellan R (1994) Non-equilibrium mass transfer between the vapor, aqueous, and solid phases in unsaturated soils during vapor extraction. *Water Resources Research* 30:355–368

- Bedeaux D, Kjelstrup S (1999) Transfer coefficients for evaporation. *Physica A* 270:413–426
- Bénet J, Jouanna P (1982) Phenomenological relation of phase change of water in a porous medium: experimental verification and measurement of the phenomenological coefficient. *International Journal of Heat and Mass Transfer* 25:1747–1754
- Bond M, Struchtrup H (2004) Mean evaporation and condensation coefficients based on energy dependent condensation probability. *Physical Review E* 70:doi:10.1103/PhysRevE.70.061,605
- Chammari A, Naon B, Cherblanc F, Bénet JC (2003) Transfert d'eau en sol aride avec changement de phase - water transport with phase change at low water content. *Comptes Rendus de Mécanique* 331:759–765
- Chammari A, Naon B, Cherblanc F, Cousin B, Bénet JC (2008) Interpreting the drying kinetics of a soil using a macroscopic thermodynamic non-equilibrium of water between the liquid and vapour phase. *Drying Technology* 26:836–843
- Couture F, Fabrie P, Puiggali J (1995) An alternative choice for the drying variables leading to a mathematically and physically well described problem. *Drying Technology* 13:519–550
- Delage P, Audiguier M, Cui Y, Howat M (1996) Microstructure of a compacted silty clay. *Canadian Geotechnical Journal* 33:150–158
- Eames I (1997) The evaporation coefficient of water : a review. *International Journal of Heat and Mass Transfer* 42:2963–2973
- Fang G (1999) Temperature measured close to the interface of an evaporating liquid. *Physical Review* 59:417–428
- Gawin D, Lefik M, Schrefler B (2001) ANN approach to sorption hysteresis within a coupled hygro-thermo-mechanical FE analysis. *International Journal for Numerical Methods in Engineering* 50:299–323
- Kjelstrup S, Bedeaux D, Inzoli I, Simon JM (2008) Criteria for validity of thermodynamic equations from non-equilibrium molecular dynamics simulations. *Energy* 33:1185– 1196
- Kuiken (1994) *Thermodynamics for irreversible processes*. Wiley, Chichester
- Leroy P, Revil A, Altmann S, Tournassat C (2007) Modeling the composition of the pore water in a clay-rock geological formation (Callovo-Oxfordian, France). *Geochimica et Cosmochimica Acta* 71:1087–1097
- Lozano A, Cherblanc F, Cousin B, Bénet JC (2008) Experimental study and modelling of the water phase change kinetics in soils. *European Journal of Soil Science* 59:939–949
- Marek R, Straub J (2001) Analysis of the evaporation coefficient and the condensation coefficient of water. *International Journal of Heat and Mass Transfer* 44:39–53
- Matsumoto M (1998) Molecular dynamics of fluid phase change. *Fluid Phase Equilibria* 144:307–314
- Meland R, Frezzotti A, Yttrhus T, Hafskjold B (2003) Nonequilibrium molecular-dynamics simulation of net evaporation and net condensation, and evaluation of the gas-kinetic boundary condition at the interphase. *Physics of Fluids* 16:223–243
- Mitchell J (1993) *Fundamentals of soil behaviour*. John Wiley and Sons, New York
- Moyne C, Perre P (1991) Processes related to drying. part i. theoretical model. *Drying Technology* 9:1135–1152

- Park S, Sposito G (2002) Structure of water adsorbed on a mica surface. *Physical Review Letters* 89:doi 10.1103/PhysRevLett.89.085,501
- Porion P, Michot L, Faugre A, Delville A (2007) Structural and dynamical properties of the water molecules confined in dense clay sediments: a study combining  $^2\text{H}$  NMR spectroscopy and multiscale numerical modeling. *Journal of Physical Chemistry C* 111:5441–5453
- Prat M (2002) Recent advances in pore-scale models for drying of porous media. *Chemical Engineering Journal* 86:153–164
- Press W, Teukolsky S, Vetterling W (1992) *Numerical recipes in C. The art of scientific computing.* Cambridge University Press
- Ruiz T, Bénét J (2001) Phase change in a heterogeneous medium: comparison between the vaporisation of water and heptane in an unsaturated soil at two temperatures. *Transport in porous media* 44:337–353
- Saix C, Devillers P, El Youssoufi M (2000) Eléments de couplage thermomécanique dans la consolidation de sols non saturés. *Canadian Geotechnical Journal* 37:308–317
- Skipper N (1998) Computer simulation of aqueous pore fluids in 2:1 clay minerals. *Mineralogical Magazine* 62:657–667
- Whitaker S (1977) Simultaneous heat, mass, and momentum transfer in porous media: a theory of drying. *Advances in Heat Transfer* 13:119–203.
- Yasuoka K, Matsumoto M, Kataoka Y (1995) Dynamics near a liquid surface: Mechanisms of evaporation and condensation. *Journal of Molecular Liquids* 65-66:329–332